Journal of Mathematics and Modeling in Finance (JMMF)
Vol. 7, No. 1, Winter & Spring 2027
Research paper

A Comparative Study of Numerical Methods for Option Pricing under Arithmetic, Geometric, and Hybrid Brownian Motion Models

Mohammad Reza Haddadi[1], **Ahmad Reza Golmohamadi**[2], **Hossein Nasrollahi**[3], **Manizheh Goudarzi**[4]

[1] Zagros Financial Research Group, Ayatollah Boroujerdi University, Boroujerd, Iran.
haddadi@abru.ac.ir

[2] Zagros Financial Research Group, Ayatollah Boroujerdi University, Boroujerd, Iran.
areza.golmohamadi@abru.ac.ir

[3] Zagros Financial Research Group, Ayatollah Boroujerdi University, Boroujerd, Iran.
hosein.nasrolahi@abru.ac.ir

[4] Zagros Financial Research Group, Ayatollah Boroujerdi University, Boroujerd, Iran.
m.goudarzi@abru.ac.ir

Abstract:
The aim of this paper is the pricing of European call options using analytical and numerical approaches. To this end, we investigated three main models: the Black-Scholes model, the Bachelier model, and the Geometric and Arithmetic Mixed Brownian Motion model. For the numerical solution of the mixed Brownian Motion model, the Crank-Nicolson method and the Euler discretization method were used. The data used in this research pertains to the stocks of “Shasta” (from April 13, 2020, to May 26, 2024) and “Ahrom” (from December 20, 2021, to May 26, 2024) traded on the Tehran Stock Exchange. We priced the options using real market data and compared the results of all three models with the observed market prices. This comparison determined that the Geometric and Arithmetic Mixed Brownian Motion model provides superior performance in option valuation.

Keywords: Black-Scholes model, Batchelor model, Crank-Nicholson Method, Brownian motion model, Options pricing.
Classification: 47H08; 47H10; 45B05.

1 Introduction

Since X_T is normally distributed, we use the moment generating function (MGF) property for a normal distribution $N(\mu, \Sigma^2)$: $E[\exp(iuZ)] = \exp(iu\mu - \frac{1}{2}u^2\Sigma^2)$.

Substituting the mean $\mu = X_t + \left(r - \frac{1}{2}\sigma^2\right)(T-t)$ and variance $\Sigma^2 = \sigma^2(T-t)$:

Option pricing models often rely on assumptions about the underlying asset's price dynamics, with geometric Brownian motion (GBM) forming the basis of the classic Black-Scholes framework. However, arithmetic Brownian motion (ABM) and various generalizations are also used, each with distinct mathematical properties and implications for pricing accuracy and risk. While Geometric Brownian Motion (GBM) allows for analytical option pricing, models based on Arithmetic Brownian

[1]Corresponding author

Received: 24/12/2025 Accepted: 22/07/2026
https://doi.org/10.22054/jmmf.2026.90616.1251

Motion (ABM) or hybrid dynamics generally require numerical methods like Monte Carlo simulations or finite difference schemes. Because hybrid models lack analytical solutions due to their complex mathematical structures, the development and optimization of efficient and accurate numerical methods are essential. Recent literature emphasizes the use of advanced mathematical tools for this purpose, such as Gegenbauer orthogonal polynomials, as well as Euler and Crank-Nicolson discretization methods [1–3, 17]. The standard in financial modeling, GBM assumes asset prices evolve multiplicatively, ensuring non-negative prices and log-normal returns. This underpins the Black-Scholes model, which provides closed-form solutions for European options and is widely used in practice [12, 14, 16, 18, 22].

The Black-Scholes model, utilizing GBM, and the Bachelier model, employing ABM, are widely acknowledged as foundational models in option pricing [5, 6, 15]. The Black-Scholes model is predicated on assumptions such as a log-normal distribution of returns and constant volatility; however, its limitation lies in its inability to effectively model stochastic volatility [10]. Conversely, the Bachelier model assumes a normal distribution of returns, which presents the limitation of enabling negative asset prices [5].

The mixed geometric and arithmetic Brownian motion model or Hybrid Brownian motion (HBM) integrates the characteristics of both the Black-Scholes and Bachelier models, thereby enhancing flexibility in modeling [11].

ABM models additive price changes, enabling negative prices, which can be suitable for certain assets (for example, interest rates, some commodities). ABM-based models, such as the Bachelier model, have recently gained attention for specific markets (for example, oil futures) and offer alternative pricing formulas, though they may violate no-arbitrage conditions in some scenarios [4].

The primary objective of this paper is to determine the price of European call options using the Black-Scholes model, the Bachelier model, and the mixed geometric and arithmetic Brownian motion model. This is achieved by utilizing data from the Shasta symbol and Ahrom as the underlying assets. Furthermore, this study aims to compare the calculated prices with market option prices to ascertain which model yields a more accurate pricing outcome.

2 Materials and Methods

In the following section, we provide the asset price dynamics that follow GBM, ABM, and HBM. A stochastic process S_t is said to follow a GBM process if its price dynamics satisfy the following stochastic differential equation:

$$dS_t = \mu S_t dt + \sigma S_t dW_t, \tag{1}$$

where W_t is a Brownian motion, μ is the constant drift, and σ is the constant volatility. The solution (1) is formulated as follows:

$$S_t = S_0 \exp(\mu t - \frac{1}{2}\sigma^2 t + \sigma W_t) \quad t > 0\ ,$$

and option pricing formula from (1) has solved by Black-Scholes [6]. The Black-Scholes model equations for the price of a European call option, C, on a non-dividend-paying stock are:

$$C = S_0 N(d_1) - K e^{-rT} N(d_2), \tag{2}$$

where the parameters d_1 and d_2 are calculated using the following expressions:

$$d_1 = \frac{\ln\left(\frac{S_0}{K}\right) + \left[r + \frac{1}{2}\left(\sigma^2\right)\right] T}{\sigma\sqrt{T}}, \tag{3}$$

$$d_2 = \frac{\ln\left(\frac{S_0}{K}\right) + \left[r - \frac{1}{2}\left(\sigma^2\right)\right] T}{\sigma\sqrt{T}} = d_1 - \sigma\sqrt{T}. \tag{4}$$

In the above equations,S_0 represents the current stock price, r is the continuously compounded risk-free rate, K is the strike price, σ is the annualized volatility (standard deviation) of the underlying asset's returns, and $N(.)$ denotes the Cumulative Distribution Function (CDF) of the standard normal distribution [9].

A stochastic process S_t is said to follow a ABM if the asset price evolves according to the following equation:

$$dS_t = \mu S_t dt + \sigma dW_t. \tag{5}$$

Option pricing formula from (5) has solved by Bachelier [5]. The payoff of a European call option on a stock with maturity date T and strike price K is as follows:

$$\max(S_T - K, 0) = (S_T - K)^+. \tag{6}$$

European Call Option Price:

$$C_t = \left(S_t - K e^{-r(T-t)}\right) N(d) + \sigma\sqrt{\frac{1 - e^{-2r(T-t)}}{2r}} n(d), \tag{7}$$

$$d = \frac{S_t - K e^{-r(T-t)}}{\sigma\sqrt{\frac{1-e^{-2r(T-t)}}{2}}}. \tag{8}$$

The parameters are defined as: $N(.)$ is the Standard Normal Cumulative Distribution Function (CDF) and $n(.)$ is the Probability Density Function (PDF). S_t is the Current Stock Price, K is the Strike Price, t is the Current Time, and T is the Maturity Time [20]. A stochastic process S_t is said to follow a HBM if the asset price evolves according to the following equation:

$$dS_t = (\mu_1 - \mu_2 S_t)dt + \sigma_1 dW_t^1 + \sigma_2 S_t dW_t^2. \tag{9}$$

We reduce equation (9) to an Stochastic Differential Equation (SDE) with a single noise term. Let $\rho \in [-1;1]$ be the correlation between W_t^1 and W_t^2, we then re-write the SDE for S_t as follows

$$dS_t = (\mu_1 - \mu_2 S_t)dt + \sqrt{\sigma_1^2 + \sigma_2^2 S_t^2 + 2\rho\sigma_1\sigma_2 S_t}dW_t, \tag{10}$$

where W_t, W_t^1, Wt^2 are Brownian motions, μ_1, μ_2 are constant drifts, and σ_1, σ_2 are constant volatilities.

The parameter ρ in equation (10) represents the correlation between the two noises in equation (9). In the special case where $\rho = \pm 1$, that is, if perfect correlation exists between the two sources of noise, the underlying model becomes complete, see [19], which then results in the following Partial Differential Equation (PDE):

$$\left\{\begin{aligned}
&\frac{\partial C}{\partial t} + rS\frac{\partial C}{\partial S}\\
&\qquad + \frac{1}{2}(\sigma_1^2 + \sigma_2^2 S_t^2 + 2\rho\sigma_1\sigma_2 S_t)\frac{\partial^2 C}{\partial S^2} - rC = 0,\\
&C(0,t) = 0, \quad \forall t,\\
&C(S,t) \sim S \quad \text{as } S \to \infty,\\
&C(S,T) = \max(S_T - K, 0).
\end{aligned}\right\} \tag{11}$$

If a model has more sources of noise ($\rho \neq \pm 1$) than risky assets, then the Meta-theorem considers it to be incomplete, see [21], which then results in the following PDE:

$$\left\{\begin{aligned}
&\frac{\partial C}{\partial t} + \left[(\mu_1 - \mu_2 S_t) - \lambda\sqrt{\sigma_1^2 + \sigma_2^2 S_t^2 + 2\rho\sigma_1\sigma_2 S_t}\right]\frac{\partial C}{\partial S}\\
&\quad + \frac{1}{2}(\sigma_1^2 + \sigma_2^2 S_t^2 + 2\rho\sigma_1\sigma_2 S_t)\frac{\partial^2 C}{\partial S^2} - rC = 0,\\
&C(0,t) = 0, \quad \forall t,\\
&C(S,t) \sim S \quad \text{as } S \to \infty,\\
&C(S,T) = \max(S_T - K, 0).
\end{aligned}\right\} \tag{12}$$

Euler discretization is a numerical method used to approximate solutions to Partial Differential Equations (PDEs). This method proves particularly useful for time-dependent PDEs, where the solution evolves over time. The method relies on the Euler scheme, which is one of the simplest numerical techniques for solving differential equations. The finite difference scheme is the most common method used to solve Partial Differential Equations (PDEs). Among these schemes, the Crank-Nicolson (CN) method stands out due to its unique properties. The CN method is importantly an average of explicit and implicit methods, combining the strengths of both approaches. This averaging makes the method superior in terms of stability, convergence, and consistency compared to purely explicit or implicit methods. For further details, refer to [7, 8].

Euler discretization for Option pricing in HBM model is implemented as follows [7]:

$$\begin{aligned} S_{t+dt} = S_t &+ \int_t^{t+dt} \big(\mu_1 - \mu_2 S_u\big)\, du \\ &+ \int_t^{t+dt} \sqrt{\sigma_1^2 + \sigma_2^2 S_u^2 + 2\,\rho\,\sigma_1\,\sigma_2\,S_u}\, dW_u. \end{aligned} \tag{13}$$

Since

$$\int_t^{t+dt} \big(\mu_1 - \mu_2 S_u\big)\, du \approx \big(\mu_1 - \mu_2 S_t\big) \int_t^{t+dt} du = \big(\mu_1 - \mu_2 S_t\big)\, dt. \tag{14}$$

Thus, we have

$$\begin{aligned} S_{t+dt} = S_t &+ \big(\mu_1 - \mu_2 S_t\big)\, dt \\ &+ \sqrt{\sigma_1^2 + \sigma_2^2 S_t^2 + 2\,\rho\,\sigma_1\,\sigma_2\,S_t}\, Z\sqrt{dt}, \end{aligned} \tag{15}$$

where Z is a standard normal variable.
The Crank-Nicolson method applies central approximation for $\frac{\partial C}{\partial t}, \frac{\partial C}{\partial S}, \frac{\partial^2 C}{\partial S^2}$ Therefore, we have the following approximation for the differential equations in (10):

$$\frac{\partial C}{\partial t} = \frac{C_m^n - C_m^{n-1}}{\Delta t} + O(\Delta t), \tag{16}$$

$$\frac{\partial C}{\partial S} = \frac{1}{2}\left(\frac{C_{m+1}^{n-1} - C_{m-1}^{n-1}}{2\Delta S} + \frac{C_{m+1}^{n} - C_{m-1}^{n}}{2\Delta S}\right) + O(\Delta S), \tag{17}$$

$$\begin{aligned} \frac{\partial^2 C}{\partial S^2} = \frac{1}{2}\Bigg(&\frac{C_{m+1}^{n-1} - 2C_m^{n-1} + C_{m-1}^{n-1}}{(\Delta S)^2} \\ &+ \frac{C_{m+1}^{n} - 2C_m^{n} + C_{m-1}^{n}}{(\Delta S)^2}\Bigg) + O((\Delta S)^2), \end{aligned} \tag{18}$$

where $C_m^n = C(n\Delta_t, m\Delta S)$. Thus, from the equation (10) we have:

$$-a_m C_{m-1}^{n-1} + (1 - b_m) C_m^{n-1} - c_m C_{m+1}^{n-1} = a_m C_{m-1}^n + (1 + b_m) C_m^n + C_{m+1}^n, \tag{19}$$

where

$$\begin{aligned} a_m = &\frac{\Delta_t}{4\Delta S^2}\left(\sigma_1^2 + \sigma_2^2 m^2 \Delta S^2 + 2\rho\sigma_1\sigma_2 m\Delta S\right) \\ &- \frac{\Delta_t}{4\Delta S}\left((\mu_1 - m\mu_2\Delta S) - \lambda\sqrt{\sigma_1^2 + \sigma_2^2 m^2 \Delta S^2 + 2\rho\sigma_1\sigma_2 m\Delta S}\right), \end{aligned} \tag{20}$$

$$b_m = -\frac{r\Delta_t}{2} - \frac{\Delta_t}{2\Delta S^2}\left(\sigma_1^2 + \sigma_2^2 m^2 \Delta S^2 + 2\rho\sigma_1\sigma_2 m\Delta S\right), \tag{21}$$

$$\begin{aligned} c_m = & \frac{\Delta_t}{4\Delta S}\left((\mu_1 - m\mu_2\Delta S) - \lambda\sqrt{\sigma_1^2 + \sigma_2^2 m^2 \Delta S^2 + 2\rho\sigma_1\sigma_2 m\Delta S}\right) \\ & + \frac{\Delta_t}{4\Delta S^2}\left(\sigma_1^2 + \sigma_2^2 m^2 \Delta S^2 + 2\rho\sigma_1\sigma_2 m\Delta S\right). \end{aligned} \tag{22}$$

The matrix of coefficients is as follows:

$$AC_{n-1} = BC_n + D_{n-1} + D_n, n = N, \dots, 1, \tag{23}$$

$$C_n = \begin{bmatrix} C_1^n \\ C_2^n \\ \vdots \\ C_{M-1}^n \end{bmatrix}, \qquad D_n = \begin{bmatrix} a_1 C_0^n \\ 0 \\ \vdots \\ 0 \\ c_{M-1} C_M^n \end{bmatrix}, \tag{24}$$

$$A = \begin{bmatrix} 1-b_1 & -c_1 & 0 & \cdots & 0 & 0 \\ -a_2 & 1-b_2 & -c_2 & \cdots & 0 & 0 \\ & -a_3 & 1-b_3 & \cdots & 0 & 0 \\ & \vdots & \vdots & \ddots & \vdots & \vdots \\ & 0 & 0 & \cdots & -a_{M-1} & 1-b_{M-1} \end{bmatrix}, \tag{25}$$

$$B = \begin{bmatrix} 1+b_1 & c_1 & 0 & \cdots & 0 & 0 \\ a_2 & 1+b_2 & c_2 & \cdots & 0 & 0 \\ & a_3 & 1+b_3 & \cdots & 0 & 0 \\ & \vdots & \vdots & \ddots & \vdots & \vdots \\ & 0 & 0 & \cdots & a_{M-1} & 1+b_{M-1} \end{bmatrix}. \tag{26}$$

3 Results and Discussion

The Black-Scholes and Bachelier models are recognized as foundational models in option pricing. The Black-Scholes model is based on assumptions such as log-normal distribution of returns and constant volatility, and its limitation is the inability to model stochastic volatility. The Bachelier model is based on the assumption of a normal distribution of returns, and its limitation is the possibility of negative prices for assets. The Geometric-Arithmetic Brownian Motion hybrid model combines the characteristics of both the Black-Scholes and Bachelier models, providing greater flexibility in modeling. The main objective of this research is to determine the price of European call options using the Black-Scholes model, the Bachelier model, and the Geometric-Arithmetic Brownian Motion hybrid model, with data from Shasta stock and Ahrom stock as the underlying asset. Additionally, it compares the obtained prices with market option prices to identify which model provides a more appropriate price.

This study utilizes daily closing price data for Shasta stock from 13 April 2020 to 26 May 2024, and for Ahrom stock from 20 December 2021 to 26 May 2024, sourced from the Tehran Stock Exchange. The time series analysis is conducted using these datasets. The daily closing price time series for Shasta and Ahrom are presented in Figures 1 and 2, respectively.

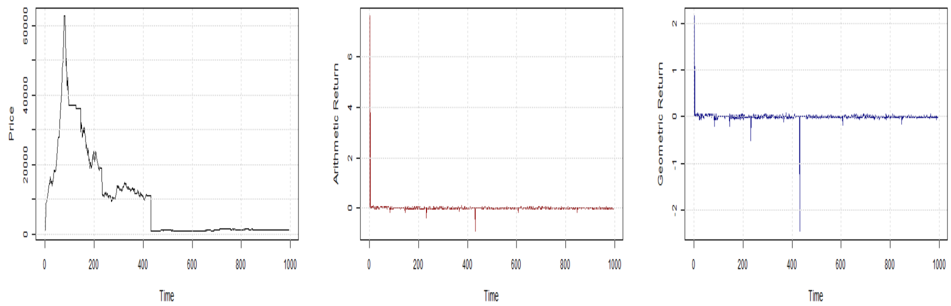

(a) Closing price of Shasta **(b)** Arithmetic Return of Shasta **(c)** Geometric Return of Shasta

Figure 1: Closing Price & Daily Returns of Shasta Stock (13 April 2020 to 26 May 2024).

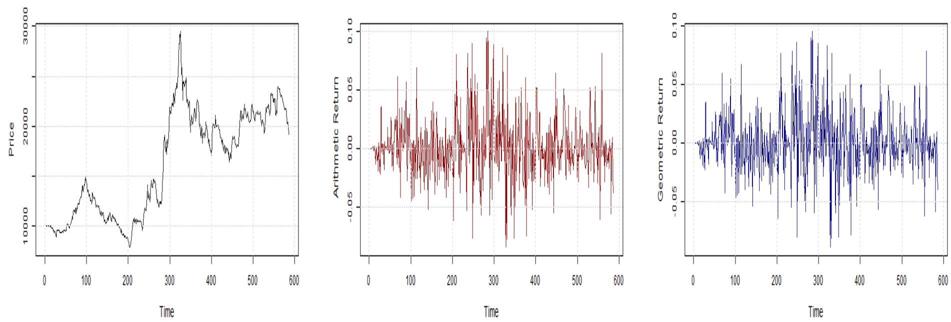

(a) Closing price of Ahrom **(b)** Arithmetic Return of Ahrom **(c)** Geometric Return of Ahrom

Figure 2: Closing Price & Daily Returns of Ahrom Stock (20 December 2021 to 26 May 2024).

Considering that the performance of different time series models can be affected by the distribution of data, descriptive statistics of the variables will be examined in Table 1 before taking any action. According to the descriptive statistics, the Ahrom stock has a more stable and favorable performance compared to Shasta; it has shown positive returns, lower risk, and a more balanced distributional behavior.

In contrast, Shasta stock has high volatility, high risk, and a greater likelihood of substantial losses.

Table 1: Descriptive statistics of daily arithmetic and geometric returns of Shasta and Ahrom stocks

Research Variable	Mean	Max	Min	Std. Dev.	Skewness	Kurtosis
Arithmetic return (Shasta)	0.00745	7.60000	-0.91363	0.24453	30.12967	938.0543
Geometric return (Shasta)	-0.000009	2.15176	-2.44918	0.10775	-3.92819	430.2867
Arithmetic return (Ahrom)	0.00146	0.09974	-0.08463	0.02645	0.46527	4.7379
Geometric return (Ahrom)	0.00111	0.09507	-0.08843	0.02628	0.32636	4.63926

Next, the normality of the daily return series of Shasta and Ahrom stocks will be examined using statistical tests. The normality test for the distribution of the arithmetic and geometric daily returns of Shasta and Ahrom stocks (Jarque-Bera test and Shapiro-Wilk test) is presented in Table 2.

Table 2: Normality test for arithmetic and geometric returns of Shasta and Ahrom stocks

Research Variable	Jarque-Bera Test		Shapiro-Wilk Test		Normality Status
	Test Statistic	p-value	Test Statistic	p-value	
Arithmetic return (Shasta)	3632549	0.0000	0.04863	0.0000	Non-normal
Geometric return (Shasta)	7556551	0.0000	0.14291	0.0000	Non-normal
Arithmetic return (Ahrom)	94.726	0.0000	0.96208	0.0000	Non-normal
Geometric return (Ahrom)	75.885	0.0000	0.96605	0.0000	Non-normal

The tests assess normality, with the null hypothesis stating the returns are normally distributed. As the p-value is below 0.05, we reject the null hypothesis, concluding that the data are non-normally distributed.

Next, to examine the type of distribution, Akaike Information Criterion (AIC) and Schwarz-Bayesian Criterion (BIC) are used.

Table 3: Distribution Analysis of Shasta Stock Arithmetic and Geometric Returns

Type of Distribution	Arithmetic Return Series		Geometric Return Series	
	Schwarz-Bayesian	Akaike	Schwarz-Bayesian	Akaike
Normal	33.71675	23.9152	-1593.787	-1603.589
Skew-normal	-650.5074	-665.2096	-1594.105	-1608.808
Student's t	-4612.1063	-4626.8085	-4559.355	-4574.058
Skew-student's t	-4613.9035	-4633.5064	-4615.564	-4635.166
Generalized Error	-6024.7360	-6039.4382	-4956.492	-4971.194
Skew-generalized Error	-4547.0097	-4566.6126	-4504.579	-4524.182
Laplace	-3923.1355	-3932.9369	-4248.274	-4258.075

Based on Table 3, for both the arithmetic and geometric returns of Shasta, the Generalized Error Distribution (GED) has the optimal fit with the lowest AIC and BIC values.

Table 4: Estimation of Parameters for the Generalized Error Distribution of Shasta Stocks

Type of Distribution	Location Parameter	Scale Parameter	Shape Parameter
Generalized Error of Arithmetic Return	0	0.4924	0.1204
Generalized Error of Geometric Return	0	0.0341	0.3717

Table 4 shows the estimation of the parameters for the Generalized Error Distribution of Shasta stocks. Based on the shape parameter value for both arithmetic and geometric returns, it is concluded that Shasta data have sharp peaks and thick tails.

Table 5: Distribution Analysis of Ahrom Stock Arithmetic and Geometric Returns

Type of Distribution	Arithmetic Return Series		Geometric Return Series	
	Schwarz-Bayesian	Akaike	Schwarz-Bayesian	Akaike
Normal	-2578.041	-2586.784	-2585.327	-2594.071
Skew-normal	-2581.048	-2594.163	-2580.379	-2593.494
Student's t	-2633.069	-2646.184	-2634.500	-2647.615
Skew-student's t	-2631.606	-2649.092	-2633.191	-2650.677
Generalized Error	-2573.073	-2586.188	-2662.063	-2675.177
Skew-generalized Error	-2653.724	-2671.210	-2577.020	-2594.507
Laplace	-2663.573	-2672.316	-2667.242	-2675.985

Based on Table 5, for both arithmetic and geometric returns, the Laplace Distribution has the optimal fit with the lowest values of AIC and BIC.

Table 6 presents the estimated parameters of the Laplace distribution fitted to Ahrom stock returns. The scale parameter estimates for both arithmetic and geometric returns indicate that, while the data exhibit symmetry, their distribution is non-normal with heavier tails than a normal distribution.

Table 6: Estimation of Parameters for the Laplace Distribution of Ahrom

Type of Distribution	Location Parameter	Scale Parameter
Laplace of Arithmetic Return	0	0.0186
Laplace of Geometric Return	0	0.0186

In Table 7 give estimation of parameters for the hybrid Brownian motion model.

Table 7: Estimation of Parameters

Parameter	μ_1	σ_1	μ_2	σ_2	ρ	λ
Shasta	0.00745	0.24453	-0.000009	0.10775	0.05629	-0.02878
Ahrom	0.00146	0.02645	0.00111	0.02628	0.01857	-0.49252

The parameter λ is commonly referred to as the market price of risk or the price of volatility risk [13]. The call option price estimated using the Black-Scholes model, the Bachelier model, and the hybrid Brownian motion model are shown in Table 8. These models were solved using the Crank-Nicolson (CN) and Euler discretization numerical methods. Table 8 also shows the percentage error ($MAPE$) of the estimated values compared to the market price for Shasta stock, where: T is the time to maturity, S is the share price, K is the strike price, and M is the market price.

Table 8: European Call Option Price for Shasta Stock and Its Error

T	S	K	M	Black-Scholes		Bachelier		Hybrid with CN		Hybrid with Euler	
				Price	% Error	Price	% Error	Price	% Error	Price	% Error
3	991	800	168	197	17	192	14	196	16	198	18
3	991	900	67	116	73	92	38	115	71	117	74
3	991	1000	5	58	1059	0	100	57	1046	57	1037
38	991	700	352	374	6	307	13	359	2	384	9
38	991	800	261	314	20	210	19	302	16	319	22
38	991	900	106	264	149	112	5	253	139	260	145
38	991	1000	31	321	613	14	52	212	584	208	573
38	991	1100	10	185	1753	0	100	177	1671	164	1541
38	991	1200	4	155	3780	0	100	148	3600	126	3055
59	991	800	216	362	67	220	2	338	57	364	68
59	991	900	129	316	145	123	3	297	130	308	139
59	991	1000	52	276	433	27	47	260	400	257	396
59	991	1100	21	242	1055	0	1000	227	986	213	914
59	991	1200	10	213	2031	3	100	200	1901	173	1633
59	991	1400	8	165	1968	0	100	154	1835	110	1283
98	991	700	391	476	21	332	14	416	6	483	23
98	991	800	302	431	42	238	20	381	26	427	41
98	991	900	238	391	64	144	39	348	46	374	57
98	991	1000	78	356	357	50	34	319	309	325	317
98	991	1100	43	325	656	0	100	292	580	281	553
98	991	1200	40	297	644	0	100	268	570	240	501

The following evaluates the error of the models based on the expiration date breakdown in Table 8. As the expiration date approaches, with only 3 days left until maturity, the market price is affected by short-term stock movements. According to Table 8, the optimal performance in this situation belongs to the Bachelier model. The combined Brownian motion model (solved with the Crank-Nicolson and Euler methods) and the Black-Scholes model have the same performance. This performance is shown graphically in Figure 3.

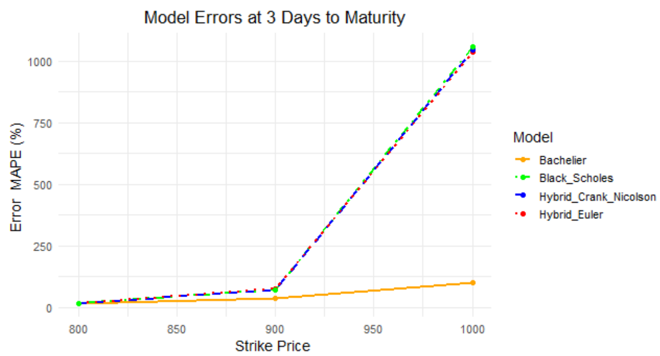

Figure 3: Comparison of the $MAPE$ errors of the models in the 3 days to maturity for Shasta

In Figure 3, the horizontal axis is the strike price (ranging from 800 to 1000) and the vertical axis is the percentage error. According to Figure3, in the entire strike price range up to about 900, the error for all models except the Bachelier model is relatively similar and minuscule. From the point 900 and above, the errors increase, and the combined Brownian motion model (solved by the Crank-Nicolson and Euler methods) and the Black-Scholes model are aligned with each other at most points. As the strike price approaches 1000, the error of the combined Brownian motion model and the Black-Scholes model increases sharply (by several times). This shows that the higher the strike price, the greater the uncertainty or prediction error. However, the error of the Bachelier model increases more gradually and with a lower slope than other models.

In the 38 days remaining until expiration, the effect of volatility gradually increases. In some cases, the Bachelier model, the combined Brownian motion model solved using the Crank-Nicolson and Euler methods, and the Black-Scholes model have similar performance. The error of the Bachelier model is smaller than that of the other models, as shown in Figure 4.

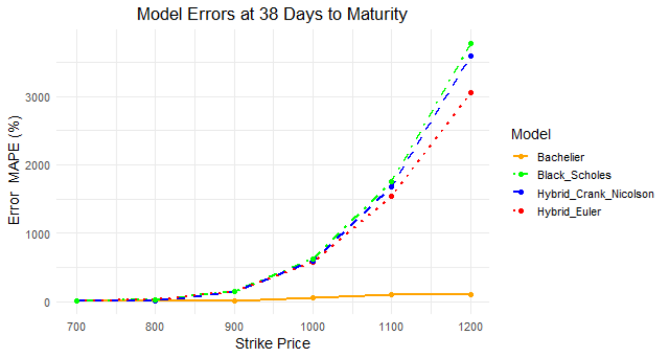

Figure 4: Comparison of the $MAPE$ errors of the models in the 38 days to maturity for Shasta

In Figure 4, the horizontal axis represents the strike price, ranging from 700 to 1200. The vertical axis indicates the percentage of error.

According to the figure, throughout the entire range of strike prices up to about 820, the errors for all models are relatively similar and minuscule. From the point of 820 and above, the errors begin to increase. The combined Brownian motion model (solved using the Crank-Nicolson and Euler methods) and the Black-Scholes model are aligned with each other at most points.

As the strike price approaches 1200, the error of the combined Brownian motion model and the Black-Scholes model sharply increases (by several times). This indicates that the rising strike price increases the uncertainty or prediction error. However, the error of the Bachelier model is smaller than that of the other models.

For the 59 days remaining until expiration, the effect of volatility gradually increases. The combined Brownian motion model (solved using the Crank-Nicolson and Euler methods) and the Black-Scholes model perform almost alike. However, the error of the Bachelier model is smaller than that of the other models, as shown in Figure 5.

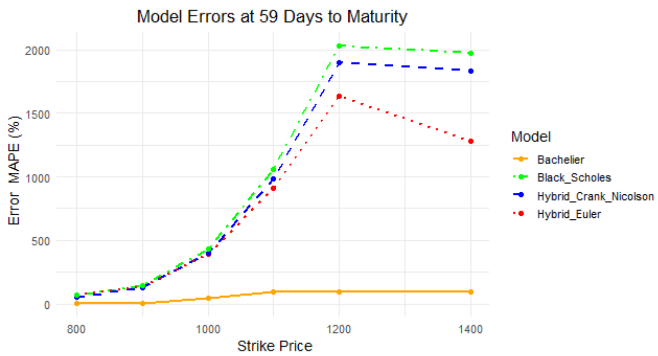

Figure 5: Comparison of the $MAPE$ errors of the models in the 59 days to maturity for Shasta

In Figure 5, the horizontal axis represents the strike price, ranging from 800 to 1400, and the vertical axis indicates the percentage of error.

According to the figure, throughout the entire range of strike prices up to about 1000, the errors for the combined Brownian motion model (solved using the Crank-Nicolson and Euler methods) and the Black-Scholes model are aligned with each other at most points.

As the strike price approaches 1200, the error of the combined Brownian motion model and the Black-Scholes model sharply increases (by several times). This indicates that the rising strike price increases the uncertainty or prediction error. However, the error of the Bachelier model is smaller than that of the other models throughout the entire range of strike prices.From the strike prices of 1200 to 1400, the errors of all models decrease.

For the 98 days remaining until expiration, as the strike price increases, the errors of the combined Brownian motion model (solved using the Crank-Nicolson and Euler methods), the Black-Scholes model, and the Bachelier model all increase. However, the error of the Bachelier model is smaller than that of the others, as shown in Figure 6.

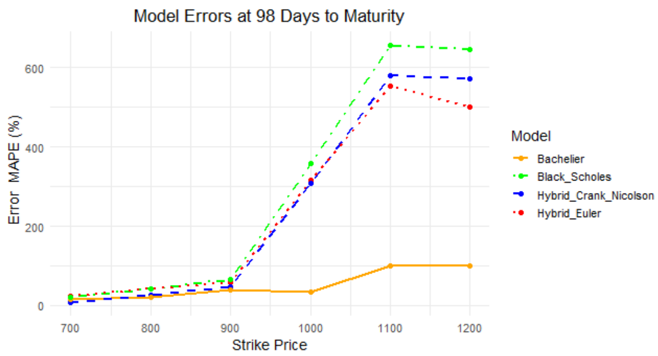

Figure 6: Comparison of the $MAPE$ errors of the models in the 98 days to maturity for Shasta

In Figure 6, the horizontal axis represents the strike price, ranging from 700 to 1200, and the vertical axis indicates the percentage of error.

According to the figure, throughout the entire range of strike prices up to about 900, the errors for the combined Brownian motion model (solved using the Euler method) and the Black-Scholes model are aligned with each other at most points and are higher than the other two models. The Bachelier model's error increases at a lower rate, and the combined Brownian motion model (solved using the Crank-Nicolson method) has the least error.

From strike prices of 900 to 1100, the errors for the combined Brownian motion model (solved using the Crank-Nicolson and Euler methods) and the Black-Scholes model sharply increase, while the error of the Bachelier model increases gently and less.

From strike prices of 1100 to 1200, the errors for the combined Brownian motion model (solved using the Crank-Nicolson and Euler methods) and the Black-Scholes model sharply decrease, while the error of the Bachelier model remains constant.

The call option price estimated using the Black-Scholes model, the Bachelier model, and the hybrid Brownian motion model are shown in Table 9. These models were solved using the Crank-Nicolson (CN) and Euler discretization numerical methods. Table 9 also presents the percentage error ($MAPE$) of the estimated values compared to the market price for Ahrom stock, where: T is the time to maturity, S is the share price, K is the strike price, and M is the market price.

Table 9: European Call Option Price for Ahrom Stock and Its Error

T	S	K	M	Black-Scholes		Bachelier		Hybrid with CN		Hybrid with Euler	
				Price	% Error	Price	% Error	Price	% Error	Price	% Error
17	19180	13000	5672	6318	11	6318	11	6280	10	6098	7
17	19180	14000	8790	5329	39	5329	39	5291	40	5110	42
17	19180	15000	5543	4340	21	4329	21	4303	22	4124	25
17	19180	16000	4672	3359	28	3350	28	3322	29	3154	32
17	19180	18000	1135	1563	37	1371	20	1533	35	1411	24
17	19180	20000	235	438	86	0	100	423	80	353	50
17	19180	22000	80	67	16	0	100	63	20	37	53
17	19180	24000	54	5	89	0	100	5	89	1	96
52	19180	14000	5491	5643	3	5631	2	5530	0.7	5021	8
52	19180	15000	4100	4704	14	4663	13	4593	12	4117	0.4
52	19180	16000	3845	3804	1	3659	3	3698	3	3264	15
52	19180	18000	1751	2236	28	1760	0.5	2150	22	1807	3
52	19180	20000	927	1124	21	0	100	1066	15	807	12
52	19180	22000	333	483	45	0	100	452	35	275	17
52	19180	24000	180	181	0.3	0	100	166	7	68	61
52	19180	26000	81	60	26	0	100	54	32	12	84
87	19180	14000	6018	5971	0.7	5926	1.5	5785	4	4999	17
87	19180	15000	8300	5083	38	4980	40	4903	41	4168	50
87	19180	16000	4200	4244	1	4033	4	4073	3	3393	19
87	19180	18000	2818	2779	1	2140	24	2636	6	2070	26
87	19180	20000	1456	1673	15	247	83	1566	7	1105	24
87	19180	22000	890	930	4	0	100	859	3	502	43
87	19180	24000	514	482	6	0	100	439	14	191	63
115	19180	18000	3172	3166	0.1	2438	23	2977	6	2232	30
115	19180	20000	2200	2065	6	578	74	1917	13	1290	41
143	19180	15000	8700	5670	35	5472	37	5384	38	4253	51
143	19180	18000	3342	3525	5	2731	18	3289	1.5	2365	29
143	19180	20000	2376	2430	2	903	62	2238	6	1445	39
143	19180	22000	1490	1611	8	0	100	1465	2	800	46

The following evaluates the error of the models based on the expiration date breakdown in Table 9. For the 17 days remaining until expiration, the comparison of call option prices using the Black-Scholes model, the Bachelier model, and the combined Brownian motion model (solved with the Crank-Nicolson and Euler discretization methods) is shown in Figure7.

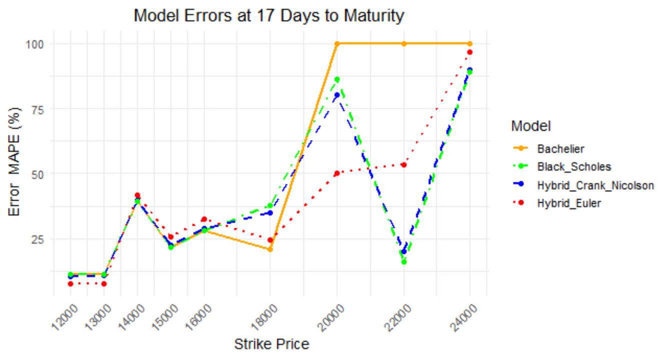

Figure 7: Comparison of the $MAPE$ errors of the models in the 17 days to maturity for Ahrom

In Figure 7, the horizontal axis represents the strike price, ranging from 12000 to 24000. The vertical axis indicates the percentage of error. According to the figure, from the strike price of 12000 to 13000, the errors of the Black-Scholes model, the Bachelier model, and the combined Brownian motion model solved with the Crank-Nicolson numerical method are similar to each other, but the error of the combined Brownian motion model solved with the Euler discretization method is lower. From the strike price of 13000 to 14000, the errors for all models increase. From the strike price of 14000 to 16000, the errors for all models first decrease and then increase. From the strike price of 16000 to 18000, the errors of the Black-Scholes model and the combined Brownian motion model solved with the Crank-Nicolson numerical method increase, while the errors of the Bachelier model and the combined Brownian motion model solved with the Euler discretization method decrease. From the strike price of 18000 to 20000, the errors for all models increase. From the strike price of 20000 to 22000, the errors of the Black-Scholes model and the combined Brownian motion model solved with the Crank-Nicolson numerical method decrease, while the error of the combined Brownian motion model solved with the Euler discretization method increases, and the error of the Bachelier model remains constant. From the strike price of 22000 to 24000, the errors of the Black-Scholes model, the combined Brownian motion model solved with the Crank-Nicolson numerical method, and the combined Brownian motion model solved with the Euler discretization method increase, while the error of the Bachelier model remains constant.

The pricing error of the call option in the 52 days remaining until expiration for the Bachelier model, the combined Brownian motion model solved with the Crank-Nicolson and Euler methods, and the Black-Scholes model is shown in Figure

8. In Figure 8, the horizontal axis represents the strike price, ranging from 14000 to 26000. The vertical axis indicates the percentage of error.

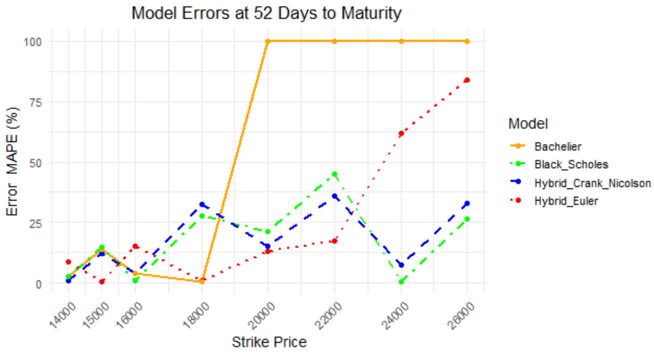

Figure 8: Comparison of the $MAPE$ errors of the models in the 52 days to maturity for Ahrom.

According to the figure, from the strike price of 14000 to 15000, the errors of the Black-Scholes model, the Bachelier model, and the combined Brownian motion model solved with the Crank-Nicolson numerical method increase, while the error of the combined Brownian motion model solved with the Euler discretization method decreases. From the strike price of 15000 to 16000, the errors of the Black-Scholes model, the Bachelier model, and the combined Brownian motion model solved with the Crank-Nicolson numerical method decrease, while the error of the combined Brownian motion model solved with the Euler discretization method increases. From the strike price of 16000 to 18000, the errors of the Black-Scholes model and the combined Brownian motion model solved with the Crank-Nicolson numerical method increase, while the errors of the Bachelier model and the combined Brownian motion model solved with the Euler discretization method decrease. From the strike price of 18000 to 20000, the errors of the Black-Scholes model and the combined Brownian motion model solved with the Crank-Nicolson numerical method decrease, while the errors of the Bachelier model and the combined Brownian motion model solved with the Euler discretization method increase. From the strike price of 20000 to 22000, the errors of the Black-Scholes model and the combined Brownian motion model solved with the Crank-Nicolson numerical method decrease, while the errors of the combined Brownian motion model solved with the Euler discretization method increase, and the error of the Bachelier model remains constant. From the strike price of 22000 to 24000, the errors of the Black-Scholes model and the combined Brownian motion model solved with the Crank-Nicolson numerical method decrease, while the error of the combined Brownian motion model solved with the Euler discretization method increases, and the error of the Bachelier model remains constant. From the strike price of 24000 to 26000, the errors of the Black-Scholes model and the combined Brownian motion model solved with the Crank-Nicolson numerical method and the combined Brownian motion model solved with the Euler discretization method increase, while the error of the Bachelier model remains constant.

The pricing error of the call option in the 87 days remaining until expiration for the Bachelier model, the combined Brownian motion model solved with the Crank-Nicolson and Euler methods, and the Black-Scholes model is shown in Figure 9.

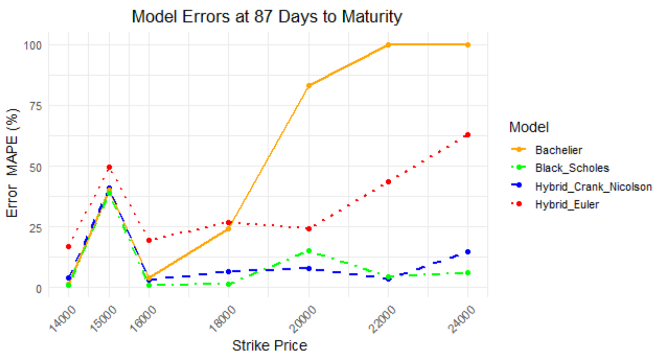

Figure 9: Comparison of the $MAPE$ errors of the models in the 87 days to maturity for Ahrom.

In Figure 9, the horizontal axis represents the strike price, ranging from 14000 to 24000. The vertical axis indicates the percentage of error. According to the figure, from the strike price of 14000 to 15000, the errors of all models increase. From the strike price of 15000 to 16000, the errors of all models decrease. From the strike price of 16000 to 18000, the errors of the Black-Scholes model and the combined Brownian motion model solved with the Crank-Nicolson numerical method and the combined Brownian motion model solved with the Euler discretization method increase slightly, while the error of the Bachelier model increases substantially. From the strike price of 18000 to 20000, the errors of the Black-Scholes model and the Bachelier model increase substantially, while the error of the combined Brownian motion model solved with the Crank-Nicolson numerical method increases slightly, and the error of the combined Brownian motion model solved with the Euler discretization method decreases slightly. From the strike price of 20000 to 22000, the errors of the Black-Scholes model and the combined Brownian motion model solved with the Crank-Nicolson numerical method decrease, while the errors of the combined Brownian motion model solved with the Euler discretization method and the error of the Bachelier model increase. From the strike price of 22000 to 24000, the error of the Black-Scholes model increases slightly, while the errors of the combined Brownian motion model solved with the Crank-Nicolson numerical method and the combined Brownian motion model solved with the Euler discretization method increase substantially, and the error of the Bachelier model remains constant.

The pricing error of the call option in the 115 days remaining until expiration for the Bachelier model, the combined Brownian motion model solved with the Crank-Nicolson and Euler methods, and the Black-Scholes model is shown in Figure 10.

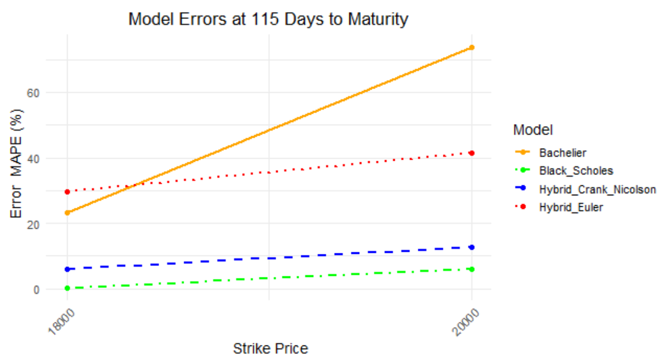

Figure 10: Comparison of the $MAPE$ errors of the models in the 115 days to maturity for Ahrom.

In Figure 10, the horizontal axis represents the strike price ranging from 18000 to 20000, while the vertical axis indicates the percentage of error. According to the figure, for the range of strike prices, the error in the Black-Scholes model and the combined Brownian motion model solved with the Crank-Nicolson and Euler numerical methods increases with a low slope, while the error of the Bachelier model increases with a high slope.

The pricing error of the call option in the 143 days remaining until expiration for the Bachelier model, the combined Brownian motion model solved with the Crank-Nicolson and Euler methods, and the Black-Scholes model is shown in Figure 11.

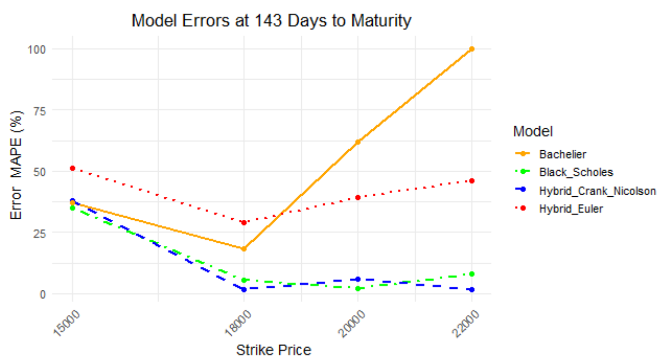

Figure 11: Comparison of the $MAPE$ errors of the models in the 143 days to maturity for Ahrom.

In Figure 11, the horizontal axis represents the strike price, ranging from 15000 to 22000. The vertical axis indicates the percentage of error. According to the figure, from the strike price of 15000 to 18000, the errors of all models decrease. From the strike price of 18000 to 20000, the error of the Black-Scholes model decreases, while the errors of the combined Brownian motion model solved with the Crank-Nicolson and Euler numerical methods and the Bachelier model increase. From the strike price of 20000 to 22000, the errors of the Black-Scholes model, the combined Brownian motion model solved with the Euler discretization method, and the Bachelier model increase, while the error of the combined Brownian motion model solved with the Crank-Nicolson method decreases.

4 Conclusion

The Black-Scholes model, using geometric Brownian motion, and the Bachelier model, employing arithmetic Brownian motion, are foundational in option pricing. The Black-Scholes model assumes a log-normal distribution of returns and constant volatility but cannot model stochastic volatility. In contrast, the Bachelier model assumes a normal distribution, which can lead to negative asset prices. A mixed model combining both approaches enhances modeling flexibility.

This research aimed to price European call options using the Black-Scholes, Bachelier, and mixed models. We used data from the Shasta and Ahrom symbols as the underlying asset. The results were compared to market prices to determine which model offered a more accurate price.

The arithmetic and geometric returns of Shasta indicate substantial volatility, with the distribution of returns being asymmetric and elongated, reflecting the presence of severe fluctuations in returns. In this symbol, the Bachelier model is recognized as the most accurate and reliable model across all time frames. The mixed Brownian motion model also performs well and shows superiority over the Black-Scholes model. These results can assist investors and analysts in selecting the appropriate model for predicting the returns of Shasta.

In contrast, the arithmetic and geometric returns of Ahrom have lower volatility compared to Shasta stocks. This means that the distribution of returns for Ahrom is more balanced and has lower variability than that of Shasta. The mixed Brownian motion model solved using the Crank-Nicolson method and the Black-Scholes model have the lowest mean error values. In this symbol, the mixed Brownian motion model solved with the Crank-Nicolson method is recognized as the most accurate and reliable model in most time frames. The Black-Scholes model also performs well, but its error standard deviation is higher. These results can aid investors and analysts in choosing the suitable model for predicting the returns of Ahrom.

Bibliography

[1] Y. E. Aghdam, H. Mesgarani, and A. Heidarvand, *Ethereum Price Prediction with a GRU-Transformer Encoder Hybrid Model*, J. Comput. Finance., (2025) 1, pp. 67-89.

[2] Y. E. Aghdam, H. Mesgarani, A. Amin, and J. F. Gómez-Aguilar, *An efficient numerical scheme to approach the time fractional black–scholes model using orthogonal gegenbauer polynomials*, Computational Economics, (2024) vol. 64, (1), pp. 211-224.

[3] Y. E. Aghdam, H. Mesgarani, and A. Amin, *Pricing of European options through a jump-diffusion technique on market prices*, International Journal of Computational Economics and Econometrics, (2026) vol. 16, (1-2), pp. 106-121.

[4] D. Alexander, M. Mo, and A. Stent, *Arithmetic Brownian motion and real options*, Eur. J. Oper. Res., (2012) vol. 219, pp. 114-122.

[5] L. Bachelier, *Théorie de la spéculation. Gauthier-Villars*, Paris, (1900).

[6] F. Black, and M. Scholes, *The pricing of options and corporate liabilities*, The Journal of Political Economy, (1973) vol. 81, (3), pp. 637-654.

[7] F. D. Rouah, *Euler and Milstein Discretization*, [Online], (2013), Available: www.FRouah.com

[8] S. E. Fadugba and C. R. Nwozo, *Crank Nicolson Finite Difference Method for the Valuation of Options*, Pacific Journal of Science and Technology, (2013) vol. 14, pp. 136-146.

[9] J. Hull, *Options, Futures, and other Derivative Securities*, Englewood Cliffs, NJ: Prentice Hall, (1993).

[10] R. C. Merton, *Theory of rational option pricing*, The Bell Journal of Economics and Management Science, (1973) vol. 4, (1), pp. 141-183.

[11] O. E. Barndorff-Nielsen and N. Shephard, *Non-Gaussian Ornstein–Uhlenbeck-based models and some of their uses in financial economics*, Journal of the Royal Statistical Society: Series B (Statistical Methodology), (2001) vol. 63, (2), pp. 167-200.

[12] C. A. Onyegbuchulem, B. O. Onyegbuchulem, and U. Alwell, *Options pricing using combination of Brownian motion with a random time component*, International Journal of Mathematical Analysis and Modelling, (2024) vol. 63, (2).

[13] O. P. Brandimarte, *Numerical Methods in Finance and Economics: A MATLAB-Based Introduction*, Hoboken, NJ: John Wiley & Sons, (2013).

[14] E. Russo, A. Leccadito, and A. Staino, *On binomial discretizations of correlated skew Brownian motions: applications to option pricing*, The European Journal of Finance, (2025), pp. 1-21

[15] A. Safdari-Vaighani, and A. Mahzarnia, *The evaluation of compound options based on RBF approximation methods*, Engineering Analysis with Boundary Elements, (2015) https://doi.org/10.1016/j.enganabound.2015.03.009

[16] M. Pourrafiee, and L. M. Mohammadi, *Comparing the different types of Markov switching model for Euro to Iran Rial exchange rate*, Journal of Mathematics and Modeling in Finance (JMMF), (2021) 1 (1), 49-58.

[17] A. Safdari-Vaighani, D. Ahmadian, R. Javid-Jahromi, *An approximation scheme for option pricing under two-state continuous CAPM*, Computational Economics, (2021) 57 (4), 1373-1385.

[18] V. Stojkoski, T. Sandev, L. Basnarkov, L. Kocarev, and R. Metzler, *Generalised Geometric Brownian Motion: Theory and Applications to Option Pricing*, Entropy, (2020) vol. 22.

[19] S. Basak, and G. Chabakauri, *Dynamic hedging in incomplete markets: a simple solution*, A simple solution, vol. 25, (6), (2012), pp. 1845-1896.

[20] S. Terakado, *On the option pricing formula based on the Bachelier model*, SSRN Electron. J., (2019).

[21] T. Björk, *Arbitrage Theory in Continuous Time, 3rd ed*, Oxford, U.K.: Oxford Univ. Press, (2009).

[22] G. Urumov, P. Chountas, and T. Chaussalet, *Fuzzy fractional Brownian motion: review and extension*, Algorithms, (2024) vol. 17, (7), pp. 289.

How to Cite: Mohammad Reza Haddadi[1], Ahmad Reza Golmohamadi[2], Hossein Nasrollahi[3], Manizheh Goudarzi[4], *A Comparative Study of Numerical Methods for Option Pricing under Arithmetic, Geometric, and Hybrid Brownian Motion Models*, Journal of Mathematics and Modeling in Finance (JMMF), Vol. 7, No. 1, Pages:127–146, (2027).